JOURNAL OF MATERIALS SCIENCE 20 (1985) 3639–3648

The effects of oxygen interaction with Pt–Rh catalytic alloys

M. RUBEL*, M. PSZONICKA
Institute of Materials Science and Engineering, Technical University of Warsaw, 02-524 Warszawa, ul. Narbutta 85, Poland

W. PALCZEWSKA
Institute of Physical Chemistry, Polish Academy of Sciences, 01-224 Warszawa, ul. Kasprzaka 44/52, Poland

The catalytic process for the oxidation of ammonia to nitric oxide by Pt–Rh alloy gauzes leads to their specific erosion and mass losses. Thus, the influence of oxygen (one of the components of the reaction mixture) upon the surface changes and mass losses of Pt90%–Rh10% and Pt95%–Rh5% alloys was studied. The reaction was investigated at 1163 and 1373 K; the oxygen pressure was 9.4×10^4 Pa. Using the XPS, AAS, SEM and EMP methods, the quantitative and qualitative composition of the volatile reaction products (PtO_2 and RhO_2) was determined, as well as the topography and chemical composition of the surface region of the gauzes. At the temperature of 1163 K, rhodium reacts with oxygen and simultaneously forms the volatile RhO_2 and the nonvolatile Rh_2O_3. This compound formation continuously stimulates rhodium diffusion to the surface along the grain boundaries. The rate of the volatile mass losses formation, at both temperatures, was also determined. The results obtained indicate that the rate of the volatile losses descreases with increasing rhodium concentration in the alloys studied.

1. Introduction

Platinum–rhodium alloys containing 5 or 10% rhodium are usually used as the catalysts for ammonia oxidation to nitric oxide. The course of this process causes the well known progressive erosion of the catalytic alloy gauzes [1–8]. This erosion leads to structural changes in the gauze wire and to the formation of the layers having a different composition to that of the initial alloy catalyst [5–7]. These changes are responsible for the state of the catalyst during the successive stages of its life, i.e. activation, activity and deactivation. Simultaneously, losses of catalyst mass are observed. According to Nowak [8], the losses are due to the formation of volatile platinum dioxide which is formed in the surface reaction between platinum contained in the catalyst with oxygen from the air–ammonia reaction mixture. The volatility of PtO_2 causes destruction of the outer layers of wires and then removal of weakly bonded crystallites, which are carried away by the gases in the reactor. These processes illustrate a reason for "mechanical" losses of the catalyst mass [1]. Then, one can suppose that oxygen is mainly responsible for the catalytic erosion of the gauzes and for their mass losses.

The essential aim of the present study was to determine, under well-defined laboratory conditions, the influence of pure oxygen upon the alloys used as catalysts in the ammonia oxidation plants. It was important to investigate simultaneously: (1) the qualitative and quantitative chemical composition of the volatile

Present address: Polish Academy of Sciences, Space Research Centre, 01-237 Warszawa, ul. Ordona 21, Poland.

0022–2461/85 $03.00 + .12

TABLE I Conditions of the NH_3 oxidation and the HCN synthesis in industry as compared with those applied in the Pt–Rh alloys oxidation in the present study

Process	Reaction mixture (vol %)	T (K)	Total pressure of the reaction mixture ($\times 10^2$ Pa)	Partial pressure of oxygen ($\times 10^2$ Pa)
Oxidation of NH_3 to NO	air–10% NH_3	1163	5065 Middle-pressure process	940
Synthesis of HCN	air–12%NH_3–13%CH_4	1400	1013	152
Oxidation of alloys under laboratory conditions	oxygen	1163	940	940
		1373	940	940
	air	1373	1013	202

materials and to find out whether they were connected only with the volatility of Pt–O compounds or with both the Pt–O and Rh–O compounds; (2) the rate of the volatile losses; (3) the changes of topography and chemical composition of the alloy surfaces after exposure to oxygen; (4) the influence of rhodium concentration upon decreases in the rate of mass losses.

2. Experimental details

The investigation was carried out with Pt90%–Rh10% and Pt95%–Rh5% alloy gauzes in the form of wire of 76 μm diameter and foils of 100 μm thickness. Alloys (99.95%) were produced in Mennica Państwowa, Poland. Before the experiments, the samples were degreased in warm acetone and then washed in boiling, concentrated hydrochloric acid (spectroscopically pure) in order to exclude contaminants – especially Groups I and II metals and iron.

The samples were oxidized, with electrolytically produced oxygen, in a Pyrex glass reactor under static conditions. The reactor tube was closed with a conical joint with two glass-coated tungsten feed-throughs to which a strip of the gauze to be investigated (5 mm × 55 mm) was spot-welded. It was heated resistively and the temperature was checked with an optical pyrometer. In the apparatus greaseless joints were used to avoid sample contamination with products of grease vapour destruction. Such contamination was detected when silicone grease was used [9].

Before the beginning of the experiments the reactor was evacuated to 1.33×10^{-2} Pa and then rinsed with oxygen.

Pt–Rh gauzes are used as catalysts in two industrial processes: i.e. oxidation of NH_3 to NO at 1073 to 1193 K and HCN synthesis from CH_4, NH_3 and air mixtures at 1373 to 1393 K. In both cases the reactant mixture contains oxygen. Therefore, the experimental conditions, i.e. temperature of the sample and oxygen pressure were carefully set so that they corresponded to the parameters of the technological processes. The fundamental data of the experimental conditions are collected in Table I and they are compared with conditions of the industrial processes, mentioned above.

The exposure times of the samples to oxygen at 1163 K were 70 and 300 h. At 1373 K the gauzes were exposed to oxygen several times during the total experimental time of 70 h, whereas the foils were oxidized in a tube oven for 200 h at 1163 K. In the case of foils, cylinder oxygen was used. It was passed through a gas purifier of a 40% water solution of KOH (p.a.), redistilled water, concentrated H_2SO_4 and dried in a column with silica gel.

During oxygen interaction with the Pt–Rh alloy samples, condensation of the volatile products of the reaction on the cooled reactor walls was observed. Simultaneously, changes of the alloy surface took place. After exposure, the condensed products of the reactions were dissolved in hot, concentrated hydrochloric acid, the solution obtained evaporated to a volume of several cm^3, and platinum and rhodium quantitatively determined by absorption atomic spectroscopy (AAS) using Jarral Ash JA 82-8111 equipment. The identification of the composition of the volatile condensed products was performed by X-ray photoelectron spectroscopy (XPS) using a Vacuum Generators ESCA-3. In order to perform this analysis the volatile

TABLE II Rates of the volatile oxide formations during the reaction of Pt–Rh alloys with molecular oxygen ($p = 9.40 \times 10^4$ Pa) or air ($p = 1.013 \times 10^5$ Pa); weight ratios m_{Pt}/m_{Rh} in the volatile oxides

Alloy	Reaction environment	Time of reaction (h)	T (K)	Rate ($\mu g\,cm^{-2}\,h^{-1}$)			m_{Pt}/m_{Rh}
				r_{PtO_2}	r_{RhO_2}	$r_{PtO_2+RhO_2}$	
Pt90%–Rh10%	Oxygen	70	1163	0.78	0.04	0.82	19.50
	Oxygen	70	1373	12.03	0.82	12.85	14.67
	Air	70	1373	4.11	0.23	4.34	17.80
Pt95%–Rh5%	Oxygen	70	1163	0.86	0.04	0.90	21.50
	Oxygen	70	1373	15.00	0.57	15.57	26.30

compounds were condensed on a gold foil (99.99%) maintained in the reactor during exposure of the Pt–Rh alloy to oxygen. The chemical shift of the 4fPt, 3dRh and 1sO photoelectron lines was checked and compared with positions of those lines for pure metals and oxygen chemisorbed on transition metals. This procedure is described elsewhere [10]. Changes in the surface topography and chemical composition of the oxidized alloys were observed by scanning electron microscopy (SEM) and electron microprobe (EMP) techniques using JEOL JSM-2 and JXA-3A equipment. The surface distributions of platinum, rhodium and oxygen were recorded. X-ray radiation was excited with a primary electron beam energy of 8.3 keV. The $M\alpha$Pt, $L\alpha$Rh and $K\alpha$O lines intensities were recorded using mica (for platinum and rhodium) and lead stearate (for oxygen) as diffraction crystals.

3. Results

3.1. The qualitative composition of the volatile oxides

The investigation of the condensed deposit carried out by the XPS method revealed that platinum and rhodium volatile dioxides were formed during reaction between alloys and oxygen. The reaction products are dark brown in colour, soluble in hot, concentrated HCl_{aq} and have a fine grain structure (below 2 nm) which was confirmed by the X-ray diffraction. Thus, one can extrapolate to the presence of the α-PtO_2 phase [11] in the volatile, condensed compounds. The presence of the β-PtO_2 phase can be excluded because this compound obtained by Berry [12] during surface oxidation of platinum at 773 to 893 K is black, orthorhombic and insoluble in acids, except hot, concentrated HBr_{aq}. At the same time the mentioned features of the reaction products confirm the presence of RhO_2. In the case of an eventual presence of Rh_2O_3, rhodium would not be detected by the AAS analysis, because this oxide is insoluble in hydrochloric acid.

3.2. The rate of formation of the volatile oxides

The quantitative determination of platinum and rhodium in oxide deposits allowed a measure of the rate of the formation of the volatile mass losses. The values obtained are shown in Table II. These results indicate a decrease in the rate with increasing rhodium concentration in the alloy sample. Moreover, the values in the last column illustrate that weight ratios m_{Pt}/m_{Rh} in the oxides formed are higher than those for initial alloy compositions.

3.3. The surface changes

Observations of the topography and chemical composition changes were carried out after alloy exposure to oxygen.

Fig. 1 shows the surface topography of Pt90%–Rh10% gauze oxidized at 1163 K for 70 h. This scanning electron micrograph is representative of the whole sample surface under examination. One can observe grain boundaries and distinct precipitations along the boundaries. Very similar topographical changes were observed on the Pt95%–Rh5% gauze surface. However, small regions of intensive etching could also be detected (Fig. 2).

The results of the EMP analysis are presented in Figs. 3 and 4 for Pt95%–Rh5% gauzes after 70 and 300 h oxidation, respectively. These show the surface composition image displayed with backscattered electrons and the surface distributions of platinum, rhodium and oxygen. The backscattered electron image (Figs. 3a and 4a) indicates that grain boundaries are enriched with elements having lower atomic number than

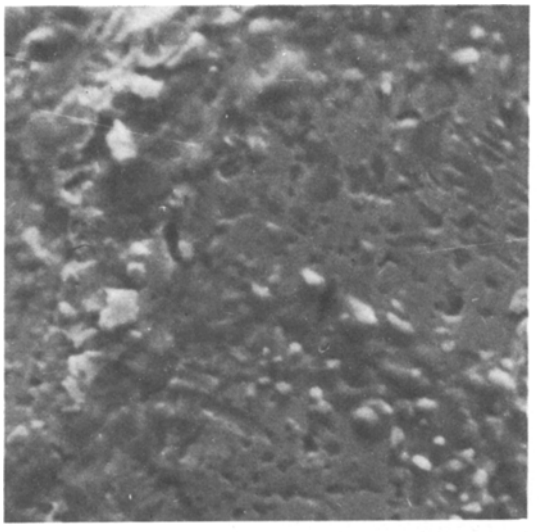

Figure 1 Topography of the Pt90%–Rh10% wire surface after 70 h oxidation at 1163 K; × 2400.

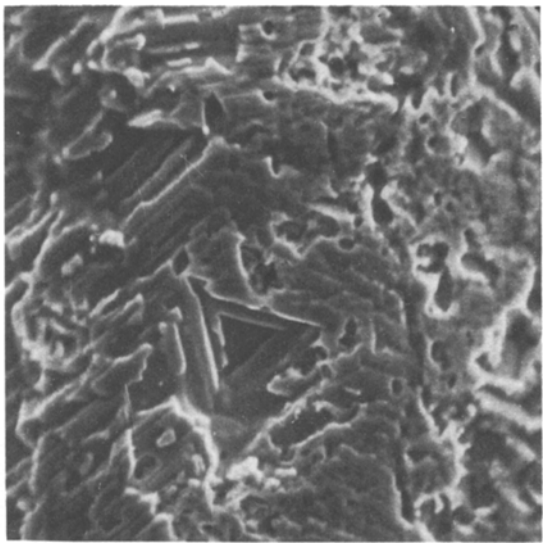

Figure 2 Topography of the Pt95%–Rh5% wire surface after 70 h oxidation at 1163 K; × 2400.

those observed on grain faces. Platinum and rhodium distributions on such a sample surface are nonuniform; the grain faces are enriched with platinum whereas at the grain boundaries the accumulation of rhodium is observed. Oxygen is recorded on the whole analysed area but grain boundaries are distinctly enriched with this element. The simultaneous appearance of rhodium could indicate the presence of the non-volatile Rh_2O_3. Similar, yet not identical, is the situation on the Pt90%–Rh10% surface (Fig. 5). Differences in the platinum and rhodium distributions are not so distinct. On the grain faces, apart from a large amount of platinum, the presence of rhodium is detected. The point analysis of the oxygen distribution revealed its greatest accumulation in the areas enriched with rhodium.

In Figs. 6a and b scanning electron micrographs of the topography of Pt95%–Rh5% foil surfaces are presented. Apart from grain boundaries and faceted regions (Fig. 6a) pits with precipitations are observed (Fig. 6b). Thus one can presume that oxide is present in such pits. The results of the EMP investigation of that area is shown in Fig. 7 and the oxide character of the bright precipitations is confirmed. This situation is also typical of the Pt90%–Rh10% foil surface.

The samples oxidized at 1373 K were investigated by SEM and EMP techniques but no distinct changes of the surfaces were detected. On the Pt90%–Rh10% alloy surface only effects due to wire recrystallization (i.e. grain boundaries appearance) were observed. The result of this observation has been previously presented [9]. Oxide precipitations were not observed and the surface distribution of alloy components was uniform.

4. Discussion

4.1. The surface changes

The observed differences of oxygen interaction with the Pt–Rh alloys exposed at 1163 and 1373 K, are connected, as one can suppose, with the stability of the surface Rh_2O_3 and the formation of volatile oxides.

The results of studies [13] of the stability of Rh_2O_3 in the Pt–Rh alloys–oxygen system, indicate that under an oxygen pressure of 9.4×10^4 Pa Rh_2O_3 decomposes at 1183 and 1223 K, in the case of the alloys containing 5 and 10% rhodium, respectively. Decomposition of the oxide in the Rh–O system occurs at 1403 K under the mentioned oxygen pressure. Thus, on the alloy surfaces heated at 1163 K the non-volatile Rh_2O_3 is stable. Simultaneously, under these conditions, the existence of surface RhO_2 is impossible because it decomposes below 923 K [11]. Yet, the possibility of surface platinum oxide formation under the experimental conditions is controversial. The results of several studies [12, 14–17] forecast the thermal decomposition of the Pt–O compounds below 890 K. Other investigators [18–20] suggest that oxygen

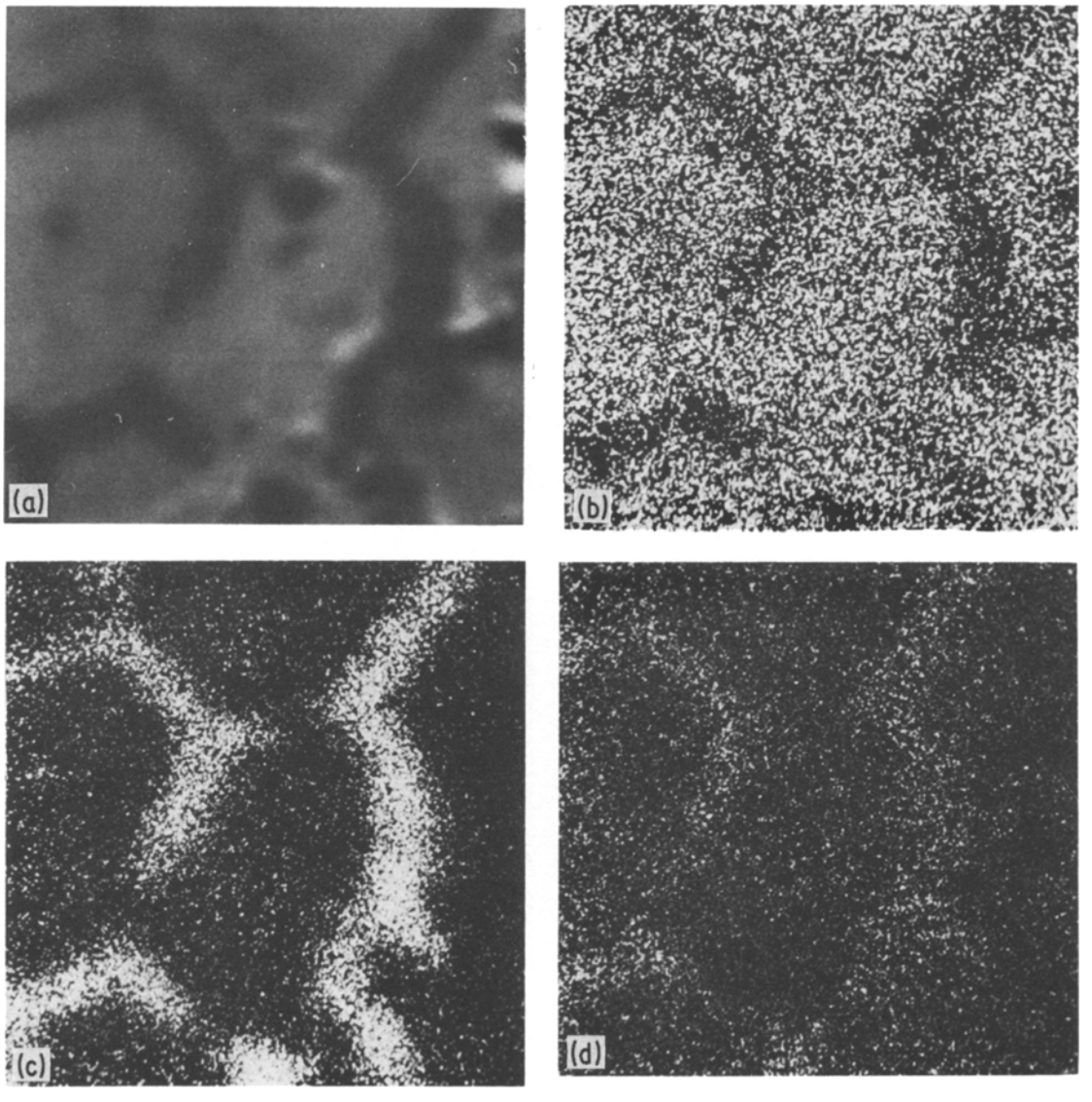

Figure 3 Results of the EMP analysis of the Pt95%–Rh5% wire surface after 70 h oxidation at 1163 K: (a) surface composition – backscattered electron image; surface distribution of: (b) platinum, (c) rhodium, (d) oxygen; × 1400.

adsorption at temperatures above 1073 K leads to subsurface oxide layer formation on the platinum single faces. However, this concept of oxide formation under such conditions was denied [21, 22] because it was proved that the investigated oxide layer contained not platinum but silicon contaminant segregated from the bulk of the sample.

The present studies carried out using the EMP method reveal that oxygen is bound especially to rhodium. This allows one to expect Rh_2O_3 on the oxidized alloy surfaces. Moreover the EMP results indicate that Rh probably diffuses along the grain boundaries to the surface and then across the grain faces. In the surface region rhodium is oxidized to the nonvolatile Rh_2O_3. This reaction causes lowering of the surface concentration of metallic rhodium. The idea of the rhodium diffusion across the surface is supported by the EMP analysis results for the Pt95%–Rh5% samples oxidized at 1163 K for 70 and 300 h (Figs. 3 and 4). The range of the regions along the grain boundaries in which rhodium enrichment is detected is 5 to 10 μm after 70 h oxidation and 15 to 45 μm after 300 h. Rhodium enrichment at grain boundaries and

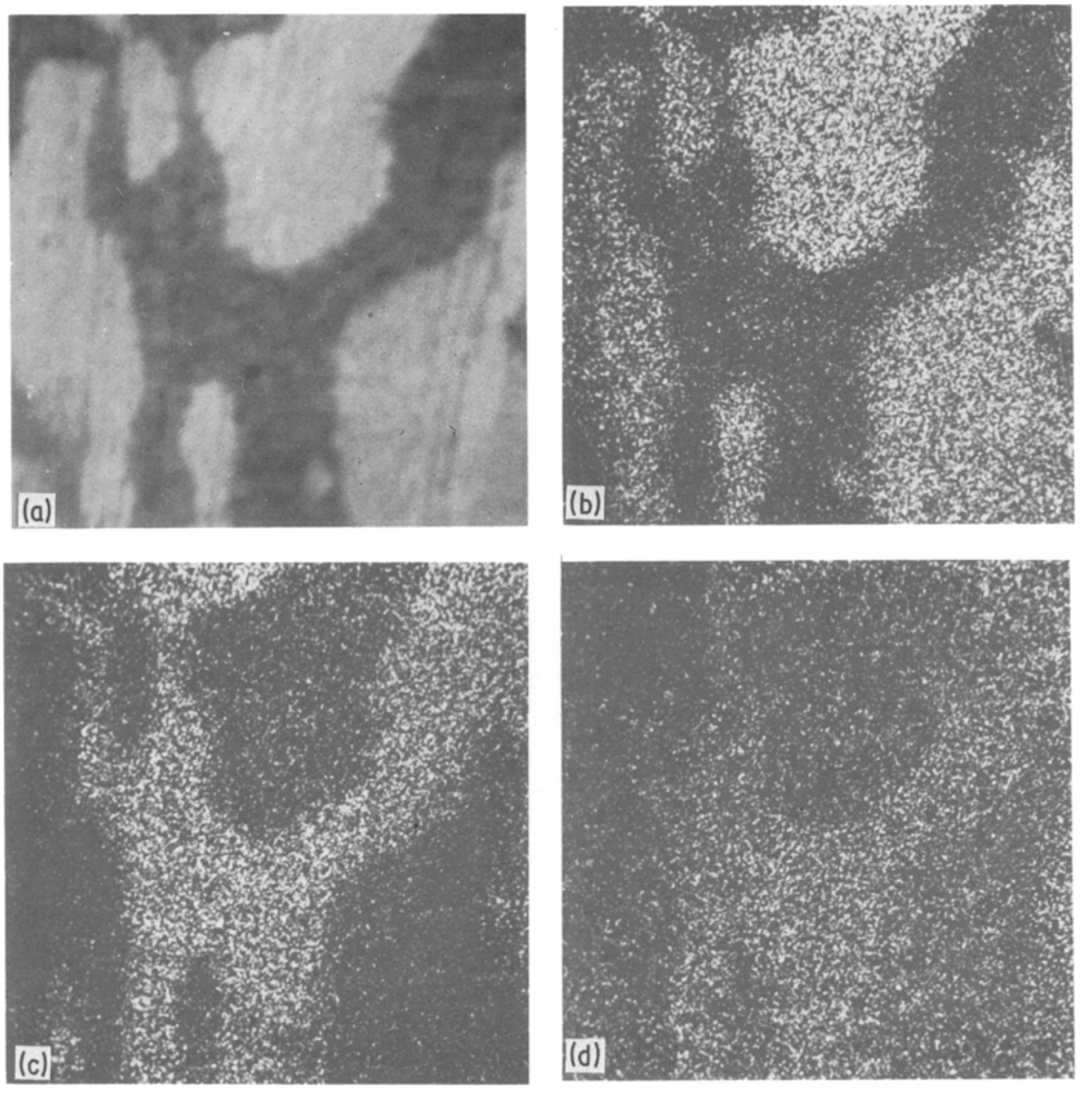

Figure 4 Results of the EMP analysis of the Pt95%–Rh5% wire surface after 300 h oxidation at 1163 K: (a) surface composition; surface distribution of: (b) platinum, (c) rhodium, (d) oxygen; × 1440.

adjacent regions is also distinct on the Pt90%–Rh10% alloy surface. However, this element is also detected on grain faces, i.e. connected with the generally higher concentration of rhodium in this alloy. In principle, precise comparison of platinum and rhodium surface concentrations after 70 and 300 h oxidation would be available by quantitative EMP analysis. However, proper performance of such analysis is impossible because of the roughness of the investigated samples. This is due to circular geometry of the samples and the effects of surface erosion. Nevertheless it was possible to analyse platinum and rhodium distributions along the cross-section of the wire. This investigation did not reveal any difference in element concentration between the core and the edge of the wire. Thus, one can suppose that only a thin layer, no more than 2 μm, is enriched with rhodium.

The observed changes in the topography and chemical compositions of the alloys oxidized under laboratory conditions at 1163 K are similar to those observed on industrial catalytic gauzes working in a NH_3 oxidation burner [2–7]. Using the EMP method Pszonicka proved a significant increase of the rhodium concentration on the surface of the gauze after its 100 h exploitation in a middle-pressure reactor. Long

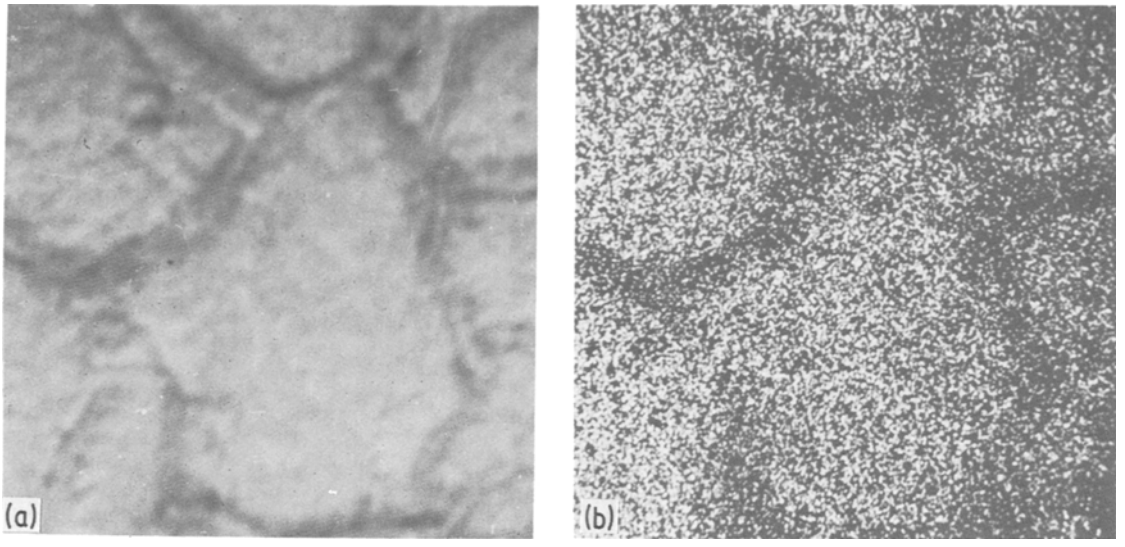

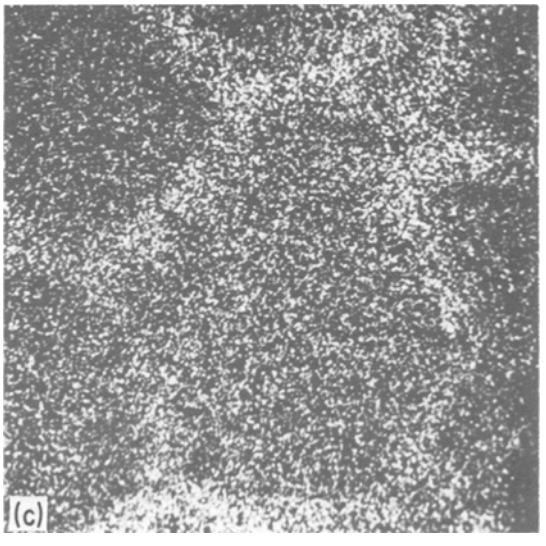

Figure 5 Results of the EMP analysis of the Pt90%–Rh10% wire surface after 70 h oxidation at 1163 K: (a) surface composition; surface distribution of: (b) platinum, (c) rhodium; × 1440.

term (about 4500 h) interaction of the NH_3 oxidation environment with alloys led to formation of layers with diversified composition and structure. The porous "sheet" of Rh_2O_3 on Pt90%–Rh10% gauze [23] and intergranular oxide net on Pt95%–Rh5% gauze [6] were observed. Also, Schmidt *et al.* [24–27], while studying oxygen influence upon composition and structure of fine-grain Pt–Rh crystallites of 2 to 20 nm deposited on SiO_2 or Al_2O_3, noticed Rh_2O_3 precipitations around the alloy particles. Similar results were obtained by McCabe and Smith [28, 29] during field ion microscopy investigation of the Pt87%–Rh13% wires oxidized in air or exposed to an air–ammonia mixture.

As mentioned previously, Pt–Rh gauzes are also applied as catalysts for HCN synthesis and during this process they undergo very intensive catalytic erosion. That was observed by the SEM technique by Schmidt and Luss [30]. However, there are no losses of the catalyst mass because the reaction occurs in a reducing atmosphere and there are no possibilities for volatile oxide formation. It seems that this is an essential reason why surface reconstruction of the catalysts for HCN synthesis is quite different to that observed on the Pt–Rh alloys oxidized at 1373 K.

4.2. The rate of formation of the volatile oxides

The results obtained indicate that the formation of nonvolatile Rh_2O_3 makes further oxidation of the wires more difficult. In effect, the rate of volatile oxide formation at 1163 K is diminished when the rhodium concentration increases. The same direction of the rate changes is noticed at 1373 K; however, the nonvolatile surface oxide does not appear under such conditions. In this case the rate decrease can be caused by differences in PtO_2 and RhO_2 vapour pressure, 9×10^{-2} and 6.5×10^{-2} Pa, respectively. These values are determined according to the Alcock and Hooper [31] equilibrium equations for dioxides. At the same time, at both experimental temperatures the weight ratios m_{Pt}/m_{Rh}

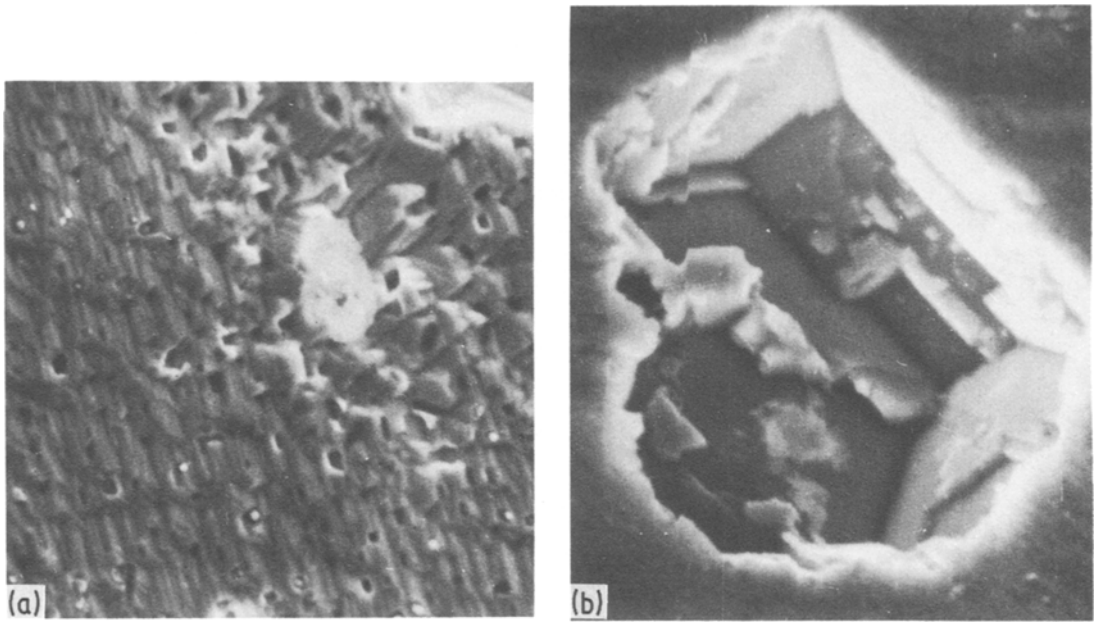

Figure 6 Topography of the Pt95%–Rh5% foil surface after 200 h oxidation in oxygen at 1163 K: (a) faceted region, (b) pit with precipitations; ×4000.

in the volatile reaction products are higher than those determined from the initial composition.

According to previous information, solid dioxides of platinum and rhodium undergo thermal decomposition under experimental conditions. However, the results of numerous studies reveal the formation of volatile PtO_2 above 1173 K [31–35] and RhO_2 above 1473 K [31, 32, 36]. These processes take place when oxides formed during surface reaction desorb immediately and then condense on the reactor walls. In the present study the volatile RhO_2 production was detected even at 1163 K. The difference between the present and the previous

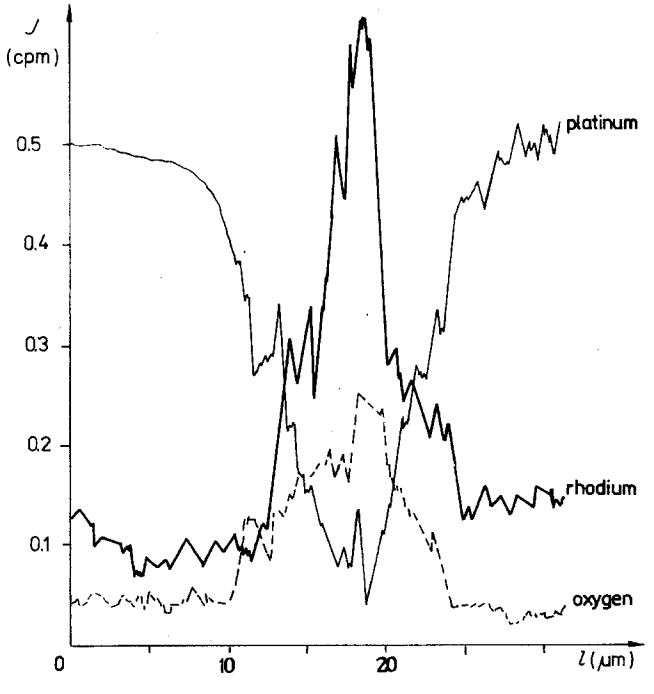

Figure 7 The distribution of elements on the Pt95%–Rh5% foil surface after 200 h oxidation in oxygen at 1163 K. $I_{Pt} \times 3 \times 10^4$, $I_O \times 3 \times 10^4$, $I_{Rh} \times 10^4$.

results is due to the use of an analytical technique for detection of volatile mass losses. Weight determination [32, 36] of the mass changes of rhodium sponges under oxidation allowed one only to detect increases of the specimen mass due to Rh_2O_3 formation (up to 1403 K, under 9.4×10^4 Pa oxygen). It is impossible to detect simultaneously the slight decrease in the sample mass due to RhO_2 volatility. Also, such determinations of mass changes of Pt–Rh sponges oxidized at 1173 and 1373 K [36] allowed investigation of the total effect only.

The measured rates of the volatile mass losses can be compared with those determined previously. For example, at 1373 K under 1.013×10^5 Pa oxygen or air Fryburg [34] observed 300 and 66 $\mu g\,cm^{-2}h^{-1}$, respectively, for ribbons of 0.287 mm width. Under the same conditions other values were obtained during oxidation of 100 to 200 cm^2 sponges (3.1 $\mu g\,cm^{-2}h^{-1}$ in oxygen [32] and 0.38 $\mu g\,cm^{-2}h^{-1}$ in air [36].

The above values differ from each other by a few orders of magnitude and also differ from those determined in the present study (Table II). One can connect these differences with the sample geometry, which influences hydrodynamic conditions of the transport of volatile species in the gas phase. This was considered by Bartlett [37] who compared the rate of the surface oxidation of platinum to PtO_2 and the rate of diffusion of this oxide molecules through the boundary layer. According to his model the specimen dimension is one of the important factors which influence the rate of the volatile compounds formation.

The mechanism of these volatile oxide formations is not quite clear. However, it seems that the essential stage of the reaction is the dissociative oxygen chemisorption. It leads to surface intermediate compound formation $[PtO]_s$ or $[PtO_2]_s$ which immediately desorb from the surface or decompose thermally. Also, it is rather doubtful that oxide formation is due to metallic atoms sublimation and their oxidation in the gas phase. The enthalpies of sublimation of both metals are about 560 kJ mol^{-1} [11] and their vapour pressures are very low (about 10^{-12} Pa at 1163 K and 10^{-9} Pa at 1373 K).

5. Conclusions

The results obtained during the present studies indicate that the character of the surface changes due to oxygen interaction with Pt–Rh alloys is similar to those observed in the case of industrial catalysts in the NH_3 oxidation process. Thus, investigation confirmed the strong oxygen influence upon catalytic corrosion of the alloys. Moreover it has revealed that losses of the catalyst masses may be attributed not only to PtO_2 but also to RhO_2 volatility. According to parallel studies of surface changes and quantitative compositions of the volatile oxides, one can propose that the following description of processes occurred on catalysts during the first stage of the oxidizing atmosphere interaction:

1. Dissociative chemisorption of oxygen on the alloy surface, leading to simultaneous oxidation of platinum to volatile PtO_2 and rhodium to nonvolatile, surface Rh_2O_3 and volatile RhO_2;

2. Rhodium diffusion to the alloy surface along the grain boundaries – this process is continuously stimulated by rhodium oxidation to Rh_2O_3 in the subsurface region.

Acknowledgements

The authors would like to thank Dr W. Skwara for AAS analysis. This work was partially supported within the Project 03.10.

References

1. H. CONNOR, *Platinum Metals Rev.* **11** (1967) 2, 60.
2. N. H. HARBORD, *ibid.* **18** (1974) 97.
3. F. SPERNER and W. HOHMANN, *ibid.* **20** (1976) 12.
4. J. P. CONTOUR, C. MOUVIER, M. HOOGEWYS and C. LECLERE, *J. Catal.* **48** (1976) 217.
5. M. PSZONICKA and T. DYMKOWSKI, *Pol. J. Chem.* **52** (1978) 121.
6. M. PSZONICKA, *ibid.* **54** (1980) 2283.
7. *Idem, ibid.* **55** (1981) 429.
8. E. J. NOWAK, *Chem. Eng. Sci.* **24** (1969) 421.
9. M. RUBEL, *J. Mater. Sci. Lett.* **4** (1985) 159.
10. M. RUBEL, J. STOCH and M. PSZONICKA, in preparation.
11. A.S.DARLING, *Inst. Met. Tev.* **18** (1973) 91.
12. R. J. BERRY, *Surface Sci.* **76** (1978) 415.
13. N. G. SCHMAHL and E. MINZL, *Z. Phys. Chem. NF* **41** (1964) 78.
14. R. J. BERRY, *Can. J. Chem.* **55** (1977) 1792.
15. M. SZUSTAKOWSKI and A. KOŁACZKOWSKI, *Chemia Stos.* **17** (1973) 127.
16. L. BREWER, *Chem. Rev.* **51** (1953) 1.
17. G. C. VAYENAS and J. N. MICHAELS, *Surface Sci.* **120** (1982) L405.
18. R. DUCROS and R. P. MERRILL, *ibid.* **55** (1976) 227.
19. R. W. McCABE and L. D. SCHMIDT, *ibid.* **60**

(1976) 85.
20. J. L. GLAND, B. A. SEXTON and G. B. FISHER, *ibid.* **95** (1980) 587.
21. H. NIEHUS and G. COMSA, *ibid.* **93** (1980) L147.
22. *Idem, ibid.* **102** (1981) L14.
23. M. PSZONICKA, *J. Catal.* **56** (1979) 472.
24. M. CHEN, T. WANG and L. D. SCHMIDT, *ibid.* **60** (1979) 356.
25. T. WANG and L. D. SCHMIDT, *ibid.* **70** (1981) 187.
26. *Idem, ibid.* **71** (1981) 411.
27. L. D. SCHMIDT and T. WANG, *Vac. Sci. Technol.* **18** (1981) 520.
28. A. R. McCABE and G. D. W. SMITH, *Platinum Metals Rev.* **27** (1983) 19.
29. A. R. McCABE and G. D. W. SMITH, in "Proceedings of the 8th International Congress on Catalysis", Vol IV, Berlin West, July 1984 (Chemie-Verlag, 1984) p. 73.
30. L. D. SCHMIDT and D. LUSS, *J. Catal.* **22** (1971) 269.
31. C. B. ALCOCK and C. W. HOOPER, *Proc. R. Soc.* **A254** (1960) 551.
32. E. RAUB and W. PLATE, *Z. Metallkde* **48** (1957) 529.
33. G. C. FRYBURG and H. M. PETRUS, *J. Electrochem. Soc.* **108** (1961) 496.
34. G. C. FRYBURG, *Trans. Met. Soc. AIME* **233** (1965) 1986.
35. H. JEHN, *J. Less-Common Metals* **78** (1981) 33.
36. C. A. KRIER and R. I. JAFFE, *ibid.* **5** (1963) 411.
37. R. W. BARTLETT, *J. Electrochem. Soc.* **114** (1967) 547.

Received 5 September
and accepted 20 November 1984